Electrostatic probe apparatus for measurements in the near-anode region of Hall thrusters

L. Dorf,[a] Y. Raitses, and N. J. Fisch
Princeton Plasma Physics Laboratory (PPPL), Princeton, New Jersey 08543

(Received 22 August 2003; accepted 27 January 2004; published 26 April 2004)

Near-anode processes in Hall-current plasma thrusters are largely uncharacterized in the experimental literature. In order to perform measurements in the near-anode region, the high potential of the anode relative to ground, small spatial variations of plasma properties, and the complicated thruster geometry are just some of the features that must be taken into consideration. A diagnostic apparatus for measurements in the near-anode region of Hall thrusters, comprising biased and emissive electrostatic probes, a high-precision positioning system, and low-noise electronic circuitry, was developed and tested. Test data for this apparatus indicate that radially inserted probes negligibly perturb the discharge. Accurate near-anode measurements of the plasma density, electron temperature, and plasma potential performed with this diagnostic have allowed the first experimental identification of the electron-repelling anode sheath predicted theoretically in Hall thrusters. © *2004 American Institute of Physics.* [DOI: 10.1063/1.1710698]

I. INTRODUCTION

In a Hall thruster[1] discharge, an axial electric field induced in a quasineutral plasma by an applied dc-voltage electrostatically accelerates ions along a coaxial channel [Fig. 1(a)]. An applied radial magnetic field in the presence of the axial electric field causes the magnetized electrons to drift in the azimuthal direction, but does not affect the unmagnetized ions. The axial flow of electrons toward the anode is therefore impeded, providing sufficient electron density for effective ionization and allowing the presence of the axial electric field in the plasma.

Over the past four decades, comprehensive experimental studies were performed on Hall thrusters.[2–11] However, near-anode processes have not received sufficient experimental scrutiny. Recent theoretical models suggest that Hall thrusters may operate with or without an electron-repelling anode sheath.[12,13] The near-anode processes might then affect the overall operation of a Hall thruster. For example, a change of the voltage drop in the anode sheath might affect anode heating, propellant ionization,[5] or the beam divergence inside and outside the thruster.

Similar to the experimental studies of the sheath and presheath in low-pressure gas discharges,[14] the plasma parameters in the near-anode region can also be studied by various electrostatic probe techniques, including single, double, and emissive probes. However, stationary probes are limited to measurements near the outer channel wall, while introducing fast reciprocating probes axially into the acceleration region, with $T_e \sim 20$ eV, can cause significant perturbations to the Hall thruster discharge, namely, fluctuations of the discharge current and its increases by up to and greater than 50%.[9,15,16] This might cause an inaccuracy of up to several volts in the measured plasma potential, which is of the order of the expected potential change over the entire near-anode region.

As we show in this article, this significant disadvantage of movable probe diagnostics vanishes if the probe is introduced radially into the near-anode region and does not pass through the acceleration region. It does not cause significant perturbations to the discharge or get severely damaged, because the electron temperature and plasma density in the near-anode region are low. For the same reason, the probe residence time is not an issue. Therefore, radial probe insertion does not require building an expensive and complex high-speed positioning system, generally associated with axial insertion of fast reciprocating probes.[17] Radial probe insertion was implemented earlier in Ref. 3 for characterization of the local plasma properties in Hall thrusters. Also noteworthy is Ref. 4, in which the probe was introduced axially through the anode and, therefore, could potentially be used for near-anode measurements. However, descriptions of the diagnostic apparatus used in these works are very concise and cannot be used to reproduce these apparatus. Besides, the reported probe measurements were mainly focused on characterizing the acceleration region in Hall thrusters and, therefore, do not provide information on the anode sheath behavior.

In this article, we present an electrostatic probe apparatus that can be used for measurements in the near-anode region of Hall thrusters, or other plasma discharges with similar geometry, discharge voltage, and near-anode plasma properties. The near-anode region in Hall thrusters is typically about 1–2 cm long. Plasma density, $n \sim 10^{10}-10^{11}$ cm^{-3}, electron temperature, $T_e \sim 3-5$ eV, and their variations in the near-anode region are smaller than in the acceleration region. The magnetic field is also much smaller, so the electron flux toward the anode is mainly affected by the electron pressure gradients, $(1/en\,dP/dz) \sim 10$ V/cm. Although the probes employed in this apparatus are not novel, this diagnostic system integrates the specific mechanical design, electronic circuitry, and measurement methods necessary for near-anode measurements, and has not been implemented previously.

[a]Electronic mail: dorf@princeton.edu

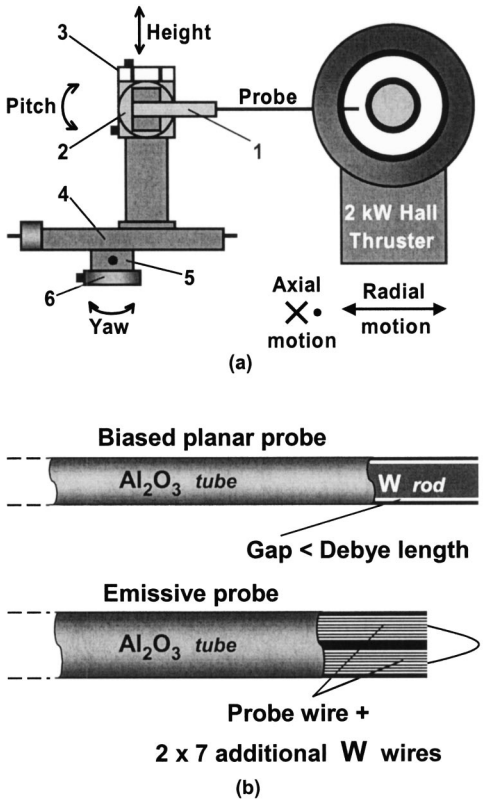

FIG. 1. Radial electrostatic probe apparatus for measurements in the near-anode region of Hall thrusters. (a) 1—probe holder, 2 and 6—manually controlled precision rotary stages for fine pitch-angle and yaw-angle adjustments, 3—precision linear stage for a fine height adjustment, 4 and 5—motor-driven $X-Y$ linear positioning stage for radial and axial probe motion. (b) Schematics of the biased and emissive electrostatic probes used in the near-anode measurements.

This article is organized as follows. Technical questions specific for near-anode measurements in Hall thrusters and other plasma discharges are discussed in Sec. II. Section III describes the diagnostic apparatus built for the characterization of a near-anode region inside a 2 kW Hall thruster. In Sec. IV, we present testing results for biased and emissive probes.

II. NEAR-ANODE MEASUREMENTS

The anode sheath thickness is typically assumed to be a few Debye lengths, where $\lambda_D \sim 0.05$ mm. Such a thin sheath does not easily accommodate probe diagnostics. The information about overall voltage drop in the sheath, however, can be obtained through probing plasma in the presheath, at several millimeters from the anode.

The radial insertion and axial motion of probes in the near-anode region of a Hall thruster require an axial slot to be machined in the outer channel wall. The sizing and placement of the slot are complicated by the relatively small size of the channel and obstacles imposed by thruster structures, for example, by the magnetic circuit.[17] One of the magnetic coils encircles the thruster channel and obstructs radial access to the acceleration region, limiting the axial motion of the probe in the near-anode region to between the anode and 14 mm from the anode for the 2 kW Hall thruster in this study. To prevent a collision between the probe and the anode, it is useful to leave a space ($\sim$1 mm) between the anode and the anode side of the slot. The minimum width of the slot, in turn, is determined by the outer diameters of the probes that will be inserted, and the maximum width is determined by the need to minimize particle losses through the slot. In particular, biased planar probes [Fig. 1(b)] need to have a sufficiently large collecting area to provide a collected probe current significantly larger than the noise. The larger probe area also allows the use of lower impedance current shunts in the probe circuit, which reduces spurious signals in the probe trace. The minimum outer diameter of emissive probes [Fig. 1(b)], alternatively, is set by the need for a simple and practical construction method.

The absolute value of the sheath voltage drop is not expected to exceed 20 V. The overall potential drop over the near-anode region is expected to be of the order of several volts. Therefore, uncertainties in interpreting the measured voltage are significantly decreased if the plasma potential is measured relative to the anode rather than to ground or cathode. In Hall thrusters, the potential of the anode relative to the ground is several hundred volts. Therefore, anode-referenced measurements require the use of isolation amplifiers, which typically have dc offsets. The dc offsets, here, are the voltages measured on the outputs of the amplifiers when the probe electronic circuit is assembled (Fig. 2) and the thruster is operating, but the probe is disconnected from the measuring circuit. In dc-offset measurements for the amplifiers in the emissive probe circuit, the probe is replaced with a 1 ohm/25 W shunt, and in dc-offset measurements for the biasing voltage amplifiers in the biased probe circuit, the biasing voltage, V_B, is set to 0 V (Fig. 2). The dc offsets of the amplifiers need to be subtracted from the corresponding recorded signals when analyzing the data from the plasma measurements. The calibration of amplifiers used in probe circuits showed that these offsets depend on the input load impedance, the discharge voltage, the mass flow rate, the heating voltage (for the emissive probe) and, especially, on the choice of reference potential. Therefore, the offsets need to be measured in each thruster operating regime and in each configuration of the probe electronic circuit—those for measuring the electron and ion parts of the probe current–voltage ($I-V$) characteristic in the case of the biased probe and those for measuring the hot and cold probe floating potentials in the case of the emissive probe (Fig. 2)—prior to performing the actual plasma measurements.

The maximum input signal for commercial isolation amplifiers is typically 10 V, which necessitates the use of voltage dividers. For floating and plasma potential measurements with a floating emissive probe, the impedance of the divider, R_{div}, must be much larger than the impedance of the probe-to-plasma interface, $R_{\mathrm{sheath}} = T_e/(e \cdot I_i^{\mathrm{sat}})$ (ratio of electron temperature to ion saturation current and electron charge), to minimize the leakage current through the probe circuit. For certain Hall thruster operating regimes, I_i^{sat} to the probe with collecting area of 3 mm^2 can be no more than several microamperes and therefore R_{sheath} can reach 1 Mohm in the near-anode plasma, yielding R_{div} must be hundreds of megaohms. In anode-referenced measurements, such a large load impedance causes the dc offset of up to hundreds of millivolts,

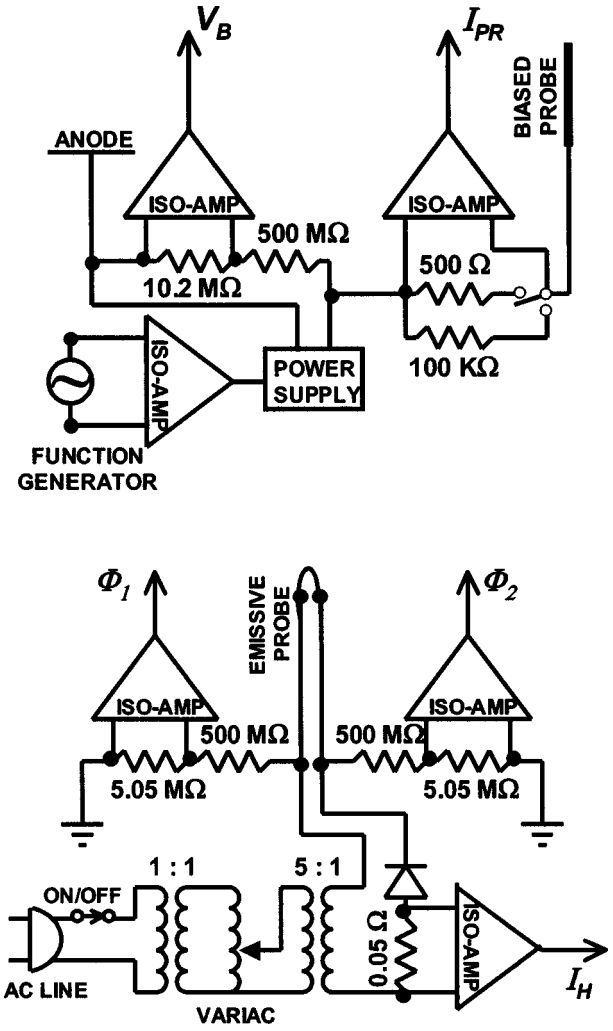

FIG. 2. Biased and emissive probe electronic circuit diagrams for measurements in the near-anode region of Hall thrusters.

which can be of the order of overall changes of the measured signal. Therefore, for emissive probe measurements, the ground appears to be a better reference than the anode, unlike that for a single biased probe.

Another source of leakage current in a probe circuit can be the plasma collected by electrical connectors, which couple the probe wire, the extension cable, and the electrical feedthrough mounted on a flange of a vacuum vessel. Wrapping all connectors in Teflon tape and closing the face of the flange with the graphite foil eliminates this problem. This was shown by placing a test wire with the tip stripped from insulation and wrapped in Teflon tape inside the vacuum vessel. The wire was connected to the emissive probe circuitry (Fig. 2) and it measured zero-floating potential at all thruster operating regimes.

Oscillations in the tens of kilohertz wave band, which are inherent to Hall thrusters, might be thought to present additional difficulties for the use of isolation amplifiers. For example, common mode rejection limitations often become important in this frequency range, potentially allowing large-amplitude noise to pass through the amplifiers. High-frequency signals applied to either or both inputs of an amplifier might also be converted to a spurious dc output signal if the input signal frequency is greater than the rated bandwidth of the amplifier. Test data for the 20 kHz amplifiers used in our apparatus indicates that, for frequencies up to 1 MHz, (a) applying the same signal with an amplitude of up to 10 V to both inputs of the amplifier results in an output signal at the level of the natural dc offset of the amplifier, and (b) applying two different signals to the inputs of the amplifier does not result in a spurious dc signal at the output. Moreover, for many sets of thruster operating parameters, the oscillations in the discharge can be significantly reduced by choosing an appropriate magnetic field configuration,[17] and these low-noise operating regimes are generally selected for performing plasma measurements. For the above reasons, the inherent oscillations should not affect the applicability of this apparatus to measurements in Hall thrusters.

III. DIAGNOSTIC APPARATUS

The 2 kW laboratory Hall thruster and test facility used in this study are described in Ref. 17. Figure 1(a) shows a radial probe apparatus for measurements in the near-anode region of a Hall discharge. The probe holder, which can accommodate up to three plain electrostatic or hot emissive probes simultaneously, is mounted on a CVI (CVI East, CT) precision rotary stage and a Newport linear stage (Newport Corp., CA) for fine pitch and height adjustment of the probe relative to the thruster channel. These manually controlled stages are assembled on a Velmex motor-driven $X-Y$ linear positioning stage (Velmex, NY), equipped with two 400 steps/rev step motors, two 40 rev/in. high precision lead screws and two 5 μm resolution Renishaw optical encoders (Renishaw, IL). This motor-driven stage is mounted on an additional CVI rotary stage for a fine yaw adjustment, which is fixed on an aluminum breadboard near the thruster mounting table. Probes can be introduced into the thruster through a 2 mm wide and 11 mm long axial slot starting at 1.5 mm from the anode, made in the outer ceramic wall of the channel. The motor-driven positioning stage allows probe motion along the slot between the inner and the outer channel walls. Control of the positioning system and the signal measurements are performed by a National Instruments, personal computer (PC)-based, data acquisition system PCI-MIO-16E-1 (National Instruments, TX).

The biased planar probe is constructed of 0.76 mm diameter thoriated tungsten rod, covered by a high-purity alumina single bore tube with outer diameter of 1.3 mm and inner diameter of 0.79 mm [Fig. 1(b)]. The probe collecting surface area, $A_{pr}=0.45$ mm^2, is much smaller than the anode cross-sectional area, $A_{an}=7700$ mm^2, so the collection of electrons by the probe, placed near the anode, does not affect the discharge. The overall probe length is 165 mm. The tungsten rod is coupled to the coaxial cable (silicon coated for vacuum compatibility) through the beryllium copper inline barrel connector. The planar tip geometry was chosen because, in the near-anode region, the $I-V$ characteristics of a planar probe appear to have more distinctive electron and ion saturation than those of a cylindrical probe. The probe sheath expansion and particle orbital motion are likely to account for this fact.[18,19]

The probe is biased relative to the anode with a KEPCO bipolar power supply BP200-1M (Kepco, NY), which is programmed with a one cycle sinusoidal signal by a PC-based function-generator connected through a Burr Brown isolation amplifier ISO124P (Fig. 2). A high-voltage vacuum switch is used to manually switch between 500 Ω and 100 kΩ shunts for measurements of electron and ion parts of the probe $I-V$ characteristic, respectively. The probe current, I_{PR}, and biasing voltage, V_B, are measured through Analog Devices isolation amplifiers AD210AN (Analog Devices, MA).

The emissive probe is constructed of a 0.1 mm diameter thorriated tungsten wire covered by a 1.6 mm diameter and 82 mm long high-purity double-bore alumina tube [Fig. 1(b)]. Each of the tube channels is filled with seven additional 0.1 mm diameter tungsten wires in order to prevent the heating of the probe aside from the tip. The probe tip protrudes from the alumina tube by 1.4 mm. The probe wires are coupled to a twisted shielded pair of 16 AWG wires (with a high-temperature Teflon insulation) through the beryllium copper connectors. A molybdenum tube extends the short alumina tube so that the overall probe length is 190 mm.

Similar to Ref. 20, the filament is heated with a 60 cycle half-wave rectified sinusoidal signal, as shown schematically in Fig. 2. During the off half-cycles of the heating voltage, the voltage drop across the probe is assumed to be zero. An additional isolation transformer is placed in front of the variac for noise reduction. The floating potentials of the probe legs, $\Phi_{1,2}$, are measured relative to the ground through isolation amplifiers AD210AN, with 10^{12} Ω input and <1 Ω output impedance. The isolation amplifiers are employed here mainly to provide impedance matching between dividers and the data acquisition system. The heating voltage can be deduced from measured floating potentials and the heating current, I_H, is measured using a 0.05 Ω current shunt and Encore Electronics isolation amplifier FL644-002 (Encore Electronics, NY) with gain set to 5.

IV. EXPERIMENTAL PROCEDURE

To test if radial probe insertion disturbs the near-anode plasma, a floating cylindrical probe (with 0.25 mm wire diameter and 3 mm uncovered tip length) was introduced into the channel at various thruster operating conditions, namely discharge voltages, V_d, from 200 to 700 V and mass flow rates, $\dot{m}$, from 2 to 5 mg/s. During the first experimental session, the probe was inserted as deep as 20 mm into the channel at several distances from the anode, $Z=2-12$ mm, and left in plasma for up to 5 min. During the second experimental session, the probe was moved from the anode side of the slot, $Z=2$ mm, to the cathode side, $Z=12$ mm, at several distances from the thruster axis, $R=37-62$ mm, i.e., from near the inner wall to near the outer wall. As can be seen from Fig. 3, the discharge current versus time characteristics indicate that the motion of the probe near the anode does not cause perturbations to the Hall thruster discharge. This leads to the conclusion that radial probe insertion is suitable for measurements in the near-anode region of a Hall thruster.

The biased and emissive probes were then used to characterize near-anode processes in the 2 kW laboratory Hall

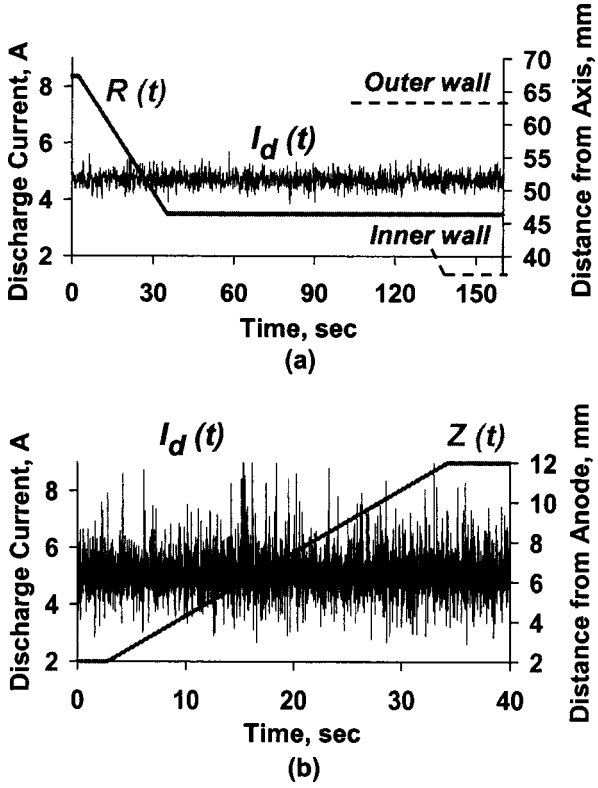

FIG. 3. Discharge current vs time characteristics for $V_d=500$ V and $\dot{m}=5$ mg/s indicate no apparent change in the discharge current level and oscillations due to the probe motion in the near-anode region of the 2 kW Hall thruster. (a) Radial insertion at $Z=2$ mm. Sampling rate=10 samples/s. (b) Axial motion at $R=55$ mm. Sampling rate=200 samples/s.

thruster. The biased planar probe data was acquired at the rate of 2000 samples per second for 6 s, in order to provide 12 sweeps of the biasing voltage (6 up and 6 down) for each measurement. A biased probe $I-V$ characteristic for $V_d=400$ V and $\dot{m}=5$ mg/s, smoothed over 40 points by using a fast Fourier transform filter and corrected for dc offsets of isolation amplifiers and voltage drop over the current shunt, is given in Fig. 4. The measured discharge current is 4.28 A, the plasma potential relative to the anode is 10.3 V, the electron temperature is 5.7 eV, and the plasma density is 4.2×10^{10} cm^{-3}. The plasma potential, φ_{pl}, and the electron saturation current, I_e^{sat}, were determined graphically by finding the kink in the electron part of a probe $I-V$ characteristic, and the electron temperature, T_e, was determined by plotting $\ln(I_{\mathrm{PR}})$ versus V_{PR} and finding a slope of the linear part of the curve.[18,19] The plasma density, n, was then deduced from the electron saturation current and the electron temperature assuming a Maxwellian electron distribution function (EDF): $n=I_e^{\mathrm{sat}}/(A_{\mathrm{pr}}\sqrt{T_e/2\pi m_e})$, where m_e is the electron mass. The statistical errors of the plasma potential, $\Delta\varphi_{\mathrm{pl}}$, and electron saturation current, $\Delta I_e^{\mathrm{sat}}$, were estimated graphically as shown in Fig. 4. The difficulty in identifying the linear part of the $\ln(I_{\mathrm{PR}})$ vs V_{PR} curve produced the relative error in the electron temperature of $\varepsilon_{T_e}\sim8-10\%$. The relative error in determining the plasma density was estimated as $\varepsilon_n=|(n^*-n)/n|\sim50\%$, where n is calculated above, and $n^*=I_d/\exp(-\varphi_{\mathrm{pl}}/T_e)\sqrt{T_e/2\pi m_e}\,A_{an})$ is the density estimated using the measured discharge current, I_d,

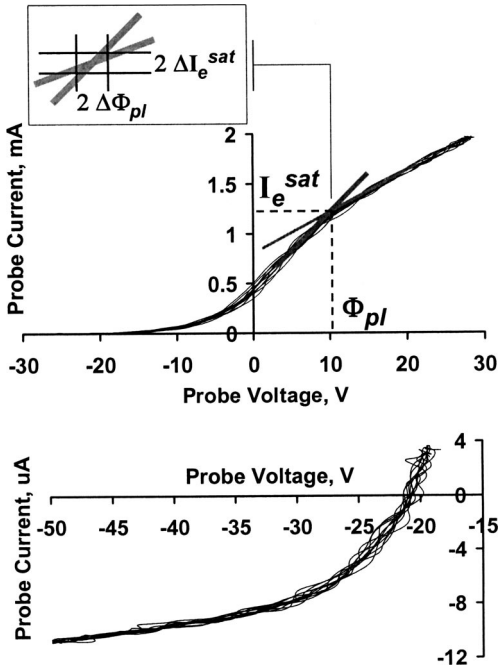

FIG. 4. Electron (above) and ion (below) parts of the biased probe $I-V$ characteristic (six up-and-down sweeps of the biasing voltage) measured in the near-anode region of the 2 kW Hall thruster. For $V_d=400$ V and $\dot{m}=5$ mg/s. At the middle of a slot, $Z=7$ mm, and channel median, $R=49$ mm. Callout box demonstrates the method for estimation of the statistical error of the plasma potential, $\Delta\Phi_{\rm pl}$, and electron saturation current, $\Delta I_e^{\rm sat}$.

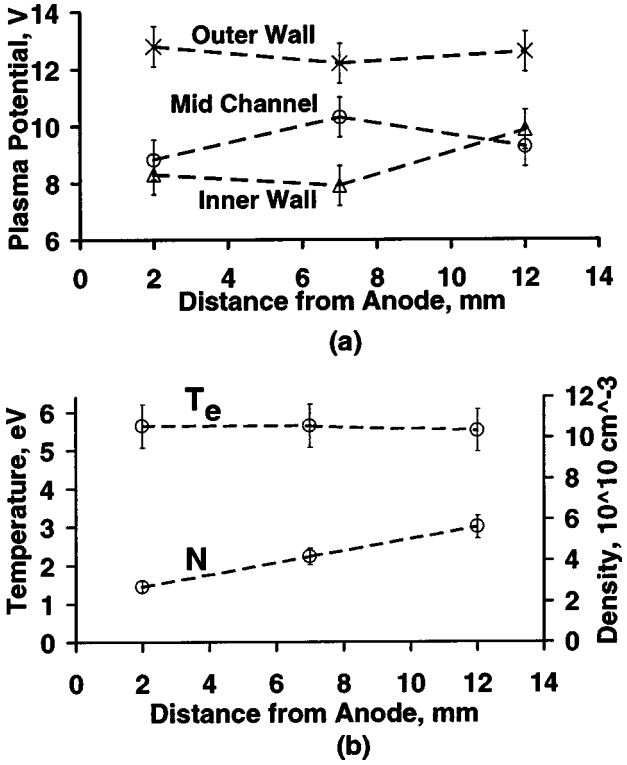

FIG. 5. Biased probe measurements in the near-anode region of the 2 kW Hall thruster. Results for $V_d=400$ V and $\dot{m}=5$ mg/s. (a) Plasma potential axial profile measured at several radial locations. Anode potential equals to zero. Shown results clearly indicate the presence of an electron-repelling anode sheath (for which the near-anode plasma potential is higher than the anode potential) predicted theoretically. (b) Electron temperature and plasma density axial profiles measured at the channel median.

along with $\varphi_{\rm pl}$ and T_e measured at 2 mm from the anode in the midpoint between the channel walls. The major source of this uncertainty is difficulty in controlling the actual collecting surface area of the probe; this issue, however, does not affect relative measurements performed with the same probe. The spatial resolution of the biased probe in the axial direction was estimated to be the outer probe diameter, 1.3 mm, since it is much greater than the estimated sheath thickness (several Debye lengths, where $\lambda_D\sim 0.05$ mm). The effects of the magnetic field and the flowing plasma are believed to be insignificant for measurements in the near-anode region of a Hall thruster.

The plasma potential, electron temperature, and plasma density axial profiles obtained with the biased probe for $V_d=400$ V and $\dot{m}=5$ mg/s are given in Fig. 5. The error bars shown in the plots of Fig. 5 were computed using the error analysis described above, and are typical for all of the experiments performed. The accuracy of the measurements performed with the described biased probe apparatus allowed successful identification of an electron-repelling anode sheath (in Fig. 5, the near-anode plasma potential is higher than the anode potential), the presence of which was predicted theoretically.[12,21] The exhaustive literature search suggests that this is the first experimental observation of the electron-repelling anode sheath in Hall thrusters.[2–11,22]

The emissive probe data was acquired at the rate of 6000 samples per second for 1 s, in order to provide 60 off half-cycles for each measurement. Figure 6 shows the emissive probe floating potential versus time characteristic, $\varphi_{\rm fl}^{\rm em}(t)$, for $V_d=300$ V and $\dot{m}=2.5$ mg/s, corrected for the dc offset of the isolation amplifier. The measured discharge current is 2.23 A, the plasma potential relative to the anode is 6.6 V, and the electron temperature is 3.9 eV. The probe floating potential saturated when the amplitude of the heating current was greater than 5.6 A, which corresponds to the heating power of approximately 12 W. The floating potential of the hot probe was averaged over 25 data points near the middle of the off half-cycle (to ensure zero heating current), and then averaged over 60 off half-cycles. The cold probe data were averaged over all 6000 points to find a floating potential. The cathode potential and the discharge voltage were measured simultaneously with the probe floating potential in order to deduce the probe potential relative to the anode.

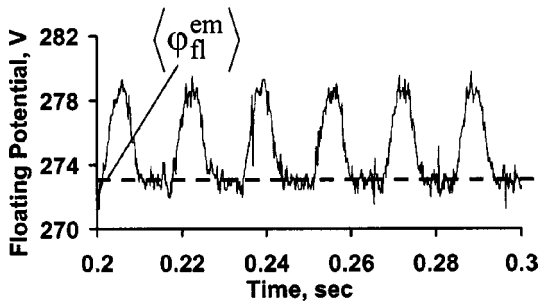

FIG. 6. Emissive probe floating potential vs time characteristic, $\Phi_2(t)$, measured in the near-anode region of the 2 kW Hall thruster. For $V_d=300$ V and $\dot{m}=2.5$ mg/s. At the middle of a slot, $Z=7$ mm, and channel median, $R=49$ mm. Heating current, $I_H=6$ A.

Due to a potential drop in the sheath and presheath formed between the probe surface and the plasma, saturated floating potential of the emissive probe appears to be smaller than the plasma potential. Following Schwager,[23] we can estimate the true plasma potential, $\varphi_{\rm pl}$, for xenon plasma as: $\varphi_{\rm pl}\approx\varphi_{\rm fl}^{\rm em}+1.5\cdot T_e$, where T_e is the electron temperature. Assuming Maxwellian EDF we can deduce T_e using a classical expression for the difference between the plasma potential and the floating potential of a cold probe, $\varphi_{\rm fl}^{\rm cl}$, which for xenon plasma becomes: $\varphi_{\rm fl}^{\rm cl}=\varphi_{\rm pl}-5.77\cdot T_e$. The final expression for $\varphi_{\rm pl}$ using measured $\varphi_{\rm fl}^{\rm em}$ and $\varphi_{\rm fl}^{\rm cl}$ can be then obtained as: $\varphi_{\rm pl}\approx 1.35\cdot\varphi_{\rm fl}^{\rm em}-0.35\cdot\varphi_{\rm fl}^{\rm cl}$.

The standard deviation of the measured plasma potential was estimated as $\sigma^{\rm pl}=1.35\cdot\sigma^{\rm em}+0.35\cdot\sigma^{\rm cl}$, where $\sigma^{\rm em}$ and $\sigma^{\rm cl}$ are the standard deviations of the floating potentials measured with the hot and the cold probes, respectively. The assumption of the Maxwellian EDF introduces an additional uncertainty in the determination of the electron temperature (and, therefore, the plasma potential), which is difficult to estimate. The standard deviation of the plasma potential measured with the emissive probe was similar to the estimated error of the plasma potential measured with the biased probe, and in all of the experiments was less than or of the order of 1 V. Measurements with the emissive probe in the near-anode region of the 2 kW laboratory Hall thruster also indicated the presence of the electron-repelling anode sheath, thus corroborating the results of the biased probe measurements.

ACKNOWLEDGMENTS

The authors would like to thank D. Staack for his contribution to preparations of the experiments. They also benefited from discussions with Dr. V. Semenov, A. Smirnov, and K. Morrison. The authors are indebted to G. D'Amico and G. Rose for excellent technical support. This work was supported by the U.S. DOE under Contract No. DE-AC02-76CH03073.

APPENDIX: CORRECTION TO THE FLOATING POTENTIAL OF THE EMISSIVE PROBE

It was shown in Ref. 24 that the increase of the emissive probe temperature does not necessarily lead to the saturation of the probe floating potential. When the ratio of the emitted current density to the collected current density, $\delta=j_{\rm em}/j_{\rm coll}$, becomes higher than the critical value, $\delta_{\rm cr}\sim 1$, the potential well is formed near the probe surface to limit the flux of emitted electrons (Fig. 7). To estimate $\varphi_{\rm pl}-\varphi_{\rm fl}^{\rm em}$, we assume that $\varphi_{\rm pl}-\varphi_{\rm min}\approx 1.5T_e/e$,[23] and that the current density of emitted electrons that reach the plasma is $j_{\rm em}^*=\delta_{\rm cr}\cdot j_{\rm coll}\sim j_{\rm coll}$. Assuming Maxwellian EDF for both emitted and collected electrons, we can write: $j_{\rm coll}=j_e^{\rm sat}\cdot\exp[e\cdot(\varphi_{\rm pl}-\varphi_{\rm min})/T_e]$ and $j_{\rm em}^*=j_{\rm em}\cdot\exp[e\cdot\Delta\varphi^*/T_{\rm pr}]$, where $j_e^{\rm sat}$ is the electron saturation current density, e is the electron charge, $\Delta\varphi^*=\varphi_{\rm fl}^{\rm em}-\varphi_{\rm min}$, and $T_{\rm pr}$ is the probe temperature. Thus, we obtain: $\varphi_{\rm pl}-\varphi_{\rm fl}^{\rm em}=1.5T_e/e-\Delta\varphi^*$ and $\Delta\varphi^*\sim\ln(4.5\cdot j_{\rm em}/j_e^{\rm sat})\cdot T_{\rm pr}/e$. Using the Richardson–Dushman's formula, $j_{\rm em}=A\cdot T_{\rm pr}^2\cdot\exp[e\cdot\varphi_w/T_{\rm pr}]$, where $A=3$ A/(cm^2 K^2) and $\varphi_w=2.65$ eV for thoriated tungsten,[24] and

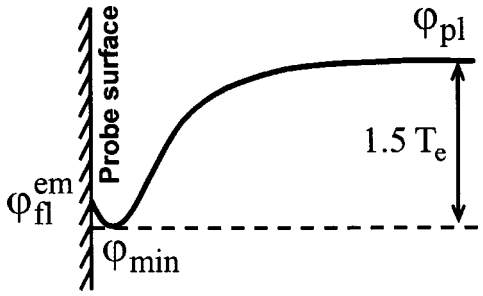

FIG. 7. Correction to the floating potential of the emissive probe: Shape of the near-probe potential profile for $\delta>\delta_{\rm cr}$.

$j_e^{\rm sat}=0.4$ A/cm^2, which is typical for the near-anode plasma in the 2 kW Hall thruster, we can finally deduce: $\Delta\varphi^*\sim\ln(5.8\cdot T_{\rm pr})\cdot T_{\rm pr}/5800-2.63$, where $T_{\rm pr}$ is in Kelvin. $\Delta\varphi^*(T_{\rm pr})$ can also be approximated with a linear function: $\Delta\varphi^*\sim T_{\rm pr}/560-2.97$. For $T_{\rm pr}=2000$ K and $T_e=5$ eV, we have $\Delta\varphi^*/(1.5T_e/e)=8\%$.

[1] A. I. Morozov and V. V. Savelyev, in *Reviews of Plasma Physics*, edited by B. B. Kadomtsev and V. D. Shafranov (Kluwer, Dordrecht, 2000), Vol. 21.
[2] A. I. Morozov, Y. V. Esinchuk, G. N. Tilinin, A. V. Trofimov, Y. A. Sharov, and G. Y. Shchepkin, Sov. Phys. Tech. Phys. **17**, 38 (1972).
[3] A. M. Bishaev and V. Kim, Sov. Phys. Tech. Phys. **23**, 1055 (1978).
[4] G. Guerrini, C. Michaut, M. Dudeck, A. N. Vesselovzorov, and M. Bacal, *Proceedings of the 25th International Electric Propulsion Conference* (Electric Rocket Propulsion Society, Cleveland, OH, 1997), IEPC Paper 1997-053.
[5] Y. Raitses, J. Ashkenazy, and M. Guelman, J. Propul. Power **14**, 247 (1998).
[6] Y. Raitses, L. Dorf, A. Litvak, and N. J. Fisch, J. Appl. Phys. **88**, 1263 (2000).
[7] J. M. Haas and A. D. Gallimore, Phys. Plasmas **8**, 652 (2001).
[8] N. B. Meezan, W. A. Hargus, Jr., and M. A. Cappelli, Phys. Rev. E **63**, 026410 (2001).
[9] Y. Raitses, M. Keidar, D. Staack, and N. J. Fisch, J. Appl. Phys. **92**, 4906 (2002).
[10] R. R. Hofer and A. D. Gallimore, *38th Joint Propulsion Conference and Exhibit* (American Institute of Aeronautics and Astronautics, Reston, VA, 2002), AIAA Paper No. 2002-4111.
[11] N. Z. Warner, J. J. Szabo, and M. Martinez-Sanchez, *Proceedings of the 28th International Electric Propulsion Conference* (Electric Rocket Propulsion Society, Cleveland, OH, 2003), IEPC Paper 2003-082.
[12] L. Dorf, V. Semenov, and Y. Raitses, Appl. Phys. Lett. **83**, 2551 (2003).
[13] M. Keidar, I. Boyd, and I. Beilis, *38th Joint Propulsion Conference and Exhibit* (American Institute of Aeronautics and Astronautics, Reston, VA, 2002), AIAA Paper 2002-4107.
[14] L. Oksuz and N. Hershkowitz, Phys. Rev. Lett. **89**, 145001 (2002).
[15] E. Chesta, C. Lam, N. Meezan, D. Schmidt, and M. Cappelli, IEEE Trans. Plasma Sci. **29**, 582 (2001).
[16] J. M. Haas and A. D. Gallimore, Rev. Sci. Instrum. **71**, 4131 (2000).
[17] Y. Raitses, D. Staack, A. Dunaevsky, L. Dorf, and N. J. Fisch, *28th International Electric Propulsion Conference* (Electric Rocket Propulsion Society, Cleveland, OH, 2003), IEPC Paper 03-0139.
[18] L. Schott, in *Plasma Diagnostics*, edited by W. Lochte-Holtgraven (Elsevier, New York, 1968), p. 669.
[19] I. H. Hutchinson, *Principles of Plasma Diagnostics* (Cambridge University Press, New York, 2002).
[20] J. R. Smith, N. Hershkowitz, and P. Coakley, Rev. Sci. Instrum. **50**, 210 (1979).
[21] E. Ahedo, P. Martinez-Cerezo, and M. Martinez-Sanches, Phys. Plasmas **8**, 3058 (2001).
[22] L. Dorf, Y. Raitses, N. J. Fisch, and V. Semenov, Appl. Phys. Lett. **84**, 1070 (2004).
[23] L. A. Shwager, Phys. Fluids B **5**, 631 (1993).
[24] T. Intrator, M. H. Cho, E. Y. Wang, N. Hershkowitz, D. Diebold, and J. DeKock, J. Appl. Phys. **64**, 2927 (1988).